RAA 2019 Vol. **19** No. **7**, 97(20pp) doi: 10.1088/1674–4527/19/7/97

http://www.raa-journal.org *http://iopscience.iop.org/raa*

Research in Astronomy and Astrophysics

Orbital parameters and period variation studies of the short-period eclipsing binaries FG Sct, VZ Lib and VZ Psc

Qiang Yue[1,2], Li-Yun Zhang⋆[1,2], Xian-Ming L. Han[1,2,3], Hong-Peng Lu[1,2], Liu Long[1,2] and Yan Yan[2,4]

[1] College of Physics/Department of Physics and Astronomy & Guizhou Provincial Key Laboratory of Public Big Data, Guizhou University, Guiyang 550025, China; *liy_zhang@hotmail.com*

[2] CAS Key Laboratory of Solar Activity, National Astronomical Observatories, Beijing 100101, China

[3] Department of Physics and Astronomy, Butler University, Indianapolis, IN 46208, USA

[4] National Astronomical Observatories, Chinese Academy of Sciences, Beijing 100101, China

Received 2018 December 19; accepted 2019 January 30

Abstract We present eight sets of new light curves for binaries FG Sct, VZ Lib and VZ Psc, which are all contact eclipsing binaries with short orbital periods. We carried out our observations from 2016 to 2017 using the 60-cm telescope administered by National Astronomical Observatories, Chinese Academy of Sciences, the Holcomb Observatory at Butler University and the SARA-CT telescope in Chile. We firstly determined the orbital parameters of FG Sct using the $O-C$ method and obtained photometric solutions utilizing the updated W-D program. We also studied its period variation and discovered that its orbital period is decreasing at a rate of 6.39($\pm$0.24) $\times 10^{-8}$ d yr^{-1}, which was likely caused by mass transfer from the primary component to the secondary component or angular momentum interchange between the two components via magnetic interactions. For VZ Lib and VZ Psc, we simultaneously analyzed their $BVRI$ light curves in conjunction with the published radial velocities. In order to obtain the orbital parameters of VZ Lib, we also analyzed its period variation and revised cyclic change, which could be attributed to either the light-time effect due to a tertiary companion or magnetic activity cycle mechanism. We derived the periods of the tertiary component of VZ Lib to be 48.7($\pm$0.1) yr or magnetic cycle to be 46.9($\pm$1.9) yr. Strong emission lines at Ca II H+K, Hα, Hβ, Hγ and Ca II IRT were detected in the LAMOST spectra of VZ Psc, which imply chromospheric activities in this binary system.

Key words: stars: binaries: eclipsing — stars: individual (FG Sct, VZ Lib, VZ Psc) — stars: starspot

1 INTRODUCTION

Short-period binaries play a significant role in research on stellar physical parameters and evolution. They are important targets for studying the period variation and their physical mechanisms, such as mass transfer from one component to another, existence of a tertiary component or magnetic activities (Applegate 1992; Hoffman et al. 2006; Zhu & Qian 2006; Zhang & Zhang 2007; Qian et al. 2017). Photometric and spectroscopic observations are crucial tools available for us to carry out these studies. Accordingly, for the purpose of better understanding their formation and evolution, further studies on the companion-star environment are considerable and necessary.

Few research works had been carried out on the short-period binary system FG Sct previously because of its position and faint brightness of 13.7 mag. FG Sct was determined to be a W UMa contact binary from photographic plates by Bradstreet (1985), and he obtained a linear ephemeris. The temperature of the hotter member was determined to be approximately that of a K3V star by Copeland et al. (1970).

VZ Lib is an eclipsing contact binary with an orbital period of 0.3582613 d. Hoffmeister (1933) found variability in light curves (LCs) of VZ Lib and the system is an eclipsing binary with low amplitude of LC variation. Claria & Lapasset (1981) obtained the photoelectric LCs, and found a difference (about 0.1 mag) between successive eclipse depths of the LC. Lu et al. (2001) carried out

⋆ Corresponding author.

spectroscopic observations, and estimated the spectral type as G0. In addition, they demonstrated that VZ Lib was a triple system with radial velocity variations in the tertiary component up to 40 km s^{-1} over a period of 1200 d. Zola et al. (2004) fitted the LC with a relative flux of 0.048 in V filter and discovered a pronounced negative O'Connell effect, signifying that secular light variation exists in this system. Rucinski & Duerbeck (2006) revised the radial velocity and found there were no obvious variations of systemic velocity. Qian et al. (2008) revised the orbital period of VZ Lib as 0.35825797 d, and found VZ Lib might be an unresolved quadruple system containing double close binary stars. Bonnardeau (2009) obtained an orbital period and inclination of the tertiary component of 34.8 yr and 11.5° respectively.

VZ Psc is recognized as a contact eclipsing binary with late-type (K2-5) components. Wolff et al. (1965) discovered that VZ Psc displayed exceptionally strong Ca II H and K emission lines, which indicated high levels of chromospheric activity and inferred high levels of magnetic activity. The variation and asymmetry of the LCs were studied by Davidge & Milone (1984), Bradstreet (1985) and Milone et al. (1985). Hrivnak & Milone (1989) obtained the radial velocity curve using the cross-correlation technique. They believed that VZ Psc was recently evolving into contact configuration from a previously wider and detached binary and identified peculiarity in the LC solution, which arises from the high degree of overcontact (74%) with a temperature difference of about 1200 K between two stars of approximately equal mass. After analyzing the period of VZ Psc, Samec (1989) concluded the period remained rather stable. Hrivnak & Milone (1989) and Barone et al. (1989) obtained new LCs and analyzed them. Their results were similar which indicated a highly overcontact configuration with large fill-out factors of 56–95%. Maceroni et al. (1990) fitted the LCs by assuming two nearly stationary dark starspots located on a hemisphere of the smaller and less massive star, and found a temperature difference between the components of about 200 K. Hrivnak et al. (1995) derived *International Ultraviolet Explorer* (*IUE*) and optical spectra, and analyzed strengths of Mg II H&K and Ca II H&K emission lines. The primary and secondary components of VZ Psc were both strongly chromospherically active. Furthermore, the secondary component was more active than the primary component (Qian et al. 2004). Ma et al. (2018) pointed out that introducing a hot spot on the primary component and adding a third companion produced the best result for their LCs. They also concluded that there is a big temperature difference of about 600 K between the primary and secondary components of VZ Psc with a high fillout factor of 94.4%.

This paper is one in a series of our published papers on magnetic activity and period variation studies of short-period eclipsing binaries (Pi et al. 2014, 2017; Lu et al. 2018). As demonstrated by these research efforts, in order to produce a comprehensive understanding of eclipsing binaries, it is necessary to observe them through multi-color CCD photometry over long periods of time. Hence, we present our new simultaneous multi-color $BVRI$ CCD photometric observations on FG Sct, VZ Lib and VZ Psc, and discuss their orbital parameters and period variations.

2 OBSERVATIONS AND DATA REDUCTION

We carried out our photometric observations of these three binaries from 2016 to 2017 using the Southeastern Association for Research in Astronomy (SARA) telescope (SARA-CT) at the Cerro Tololo Inter-American Observatory. The primary mirror for this telescope has a diameter of 0.61 meters. The CCD resolution is 1024×1024 pixels. We observed FG Sct on 2016 May 28 and 2016 Jun 21, VZ Psc on 2016 Sep 1 and 2017 Aug 21, and VZ Lib on 2016 Jun 28, 2016 Jul 1, 2016 Jul 7, 2017 May 26, 2017 May 28 and 2017 Jun 3. The images were processed using the IRAF[1] package with trimming, bias-substraction, flat-field correction, cosmic-ray removal, flat-field correction and aperture photometry.

We also observed VZ Psc using the Holcomb Observatory located at Butler University in Indianapolis, Indiana, USA on 2017 Aug 21 and 2017 Aug 24. This telescope is a 0.952 meter Cassegrain telescope. It has a field of view of about $18.1' \times 18.1'$ with a CCD resolution of 2048×2048 pixels. We processed these images using MaximDL in the standard fashion. Moreover, we also made use of the 60-cm telescope located at Xinglong Station, administered by National Astronomical Observatories, Chinese Academy of Sciences for the observations on 2017 Oct 13 and 2017 Oct 16. This telescope has an effective aperture of 60 cm and is equipped with Johnson $UBVRI$ filters. We processed all observed CCD images by applying IRAF in the standard fashion in the same way as mentioned before.

Details on our observations of these three binaries are listed in Table 1, including the names of our objects, comparison stars and check stars, exposure times, and their magnitudes. The differential magnitudes between our tar-

[1] IRAF is distributed by the National Optical Astronomy Observatories, which are operated by the Association of Universities for Research in Astronomy, Inc., under cooperative agreement with the National Science Foundation.

Table 1 Observation Log

Target	Name	Exposure Time (s) ($BVRI$)	RA(2000) and Dec(2000)	Mag$_B$	Mag$_V$
Variable	VZ Psc	60, 20, 10, 10	23 27 48.39; +04 51 24.0	11.39	10.274
Comparison	GSC 00581–00102	60, 20, 10, 10	23 27 23.55; +04 52 37.2	11.85	10.89
Check	GSC 00581–00102	60, 20, 10, 10	23 27 19.68; +04 53 49.9	11.85	10.89
Variable	VZ Lib	20, 15, 10, 10	15 31 51.76; –15 41 10.2	11.04	10.27
Comparison	GSC 06184–01101	20, 15, 10, 10	15 31 18.26; –15 45 59.0	9.94	9.45
Check	GSC 06184–00385	20, 15, 10, 10	15 31 31.57; –15 43 06.2	-	-
Variable	FG Sct	90, 60, 45, 45	18 45 03.65; –06 06 15.6	13.66	-
Comparison	2MASS J18443471–0556213	90, 60, 45, 45	18 44 34.70; –05 56 21.0	12.60	11.48
Check	2MASS J18460282–0636428	90, 60, 45, 45	18 46 00.99; –06 35 32.7	11.42	10.96

Table 2 Newly Obtained LC Minimum Times for the Three Short-period Eclipsing Binaries

Star name	HJD (24,+)$_B$	Error$_B$	HJD (24,+)$_V$	Error$_V$	HJD (24,+)$_R$	Error$_R$	HJD (24,+)$_I$	Error$_I$	Mean ($BVRI$)	Error	P/S
FG Sct	57536.77420	0.00435	57536.77457	0.00241	57536.77452	0.00228	57536.77472	0.00151	57536.77450	0.00264	S
	57536.90993	0.00152	57536.90986	0.00441	57536.90978	0.00299	57536.91022	0.00361	57536.90995	0.00313	P
	57560.85726	0.03044	57560.85665	0.01155	57560.85567	0.01108	57560.85659	0.00102	57560.85654	0.01352	S
	57560.72167	0.01731	57560.71991	0.00891	57560.71956	0.00659	57560.72038	0.00397	57560.72038	0.00920	P
VZ Psc	57632.67969	0.00132	57632.67966	0.00056	57632.67957	0.00182	57632.68014	0.00019	57632.67976	0.00097	S
	57632.80972	0.00059	57632.81015	0.00032	57632.80959	0.00024	57632.80933	0.00022	57632.80970	0.00034	P
	57986.81346	0.00172	57986.81456	0.00168	57986.81469	0.00034	57986.81499	0.00047	57986.81443	0.00105	P
	-	-	-	-	58042.98615	0.00433	58042.98537	0.00366	58042.98576	0.00400	P
	-	-	58043.11032	0.00042	58043.11539	0.00015	58043.11682	0.00038	58043.11418	0.00032	S
	57989.68283	0.00252	57989.68246	0.00212	57989.68404	0.00075	57989.68347	0.00105	57989.68321	0.00161	P
	57989.82005	0.00615	57989.82075	0.00471	57989.82081	0.00451	57989.81847	0.00368	57989.82002	0.00476	S
VZ Lib	57901.66902	0.00037	57901.66912	0.00017	57901.66921	0.00031	57901.66914	0.00026	57901.66912	0.00028	P
	57901.48941	0.00018	57901.48921	0.00021	57901.48884	0.00041	57901.48909	0.00041	57901.48913	0.00030	S
	57907.76134	0.00093	57907.76077	0.00069	57907.76076	0.00056	57907.76043	0.00074	57907.76083	0.00073	P
	57901.66902	0.00037	57901.66912	0.00017	57901.66921	0.00031	57901.66914	0.00026	57901.66912	0.00028	P
	57901.48941	0.00018	57901.48921	0.00021	57901.48884	0.00041	57901.48909	0.00041	57901.48913	0.00030	S

Notes: P – primary, S – secondary.

get stars and their comparison stars versus Heliocentric Julian Dates (HJDs) are published in electronic format. Our $BVRI$ LCs for these three binaries are plotted in Figure 1.

The Large Sky Area Multi-object Fiber Spectroscopic Telescope (LAMOST) has facilitated research on large amounts of low-dispersion spectra for many eclipsing binaries (Qian et al. 2017; Zhang et al. 2018). We acquired one spectrum of VZ Psc from the LAMOST website (Luo et al. 2015) on 2013 Sep 25. We also procured a second spectrum of VZ Psc on 2017 Dec 3 using the Yunnan Faint Object Spectrograph and Camera (YFOSC) at the Lijiang 2.4 m telescope, operated by Yunnan Observatories, Chinese Academy of Sciences (Fan et al. 2015). The YFOSC has a blue sensitive CCD with resolution of 2048 $\times$ 4608 pixels. We processed this spectrum employing the standard procedures (Lu et al. 2018) in IRAF and calibrated the wavelength with a Th-Ar lamp. The spectra are displayed in Figure 2.

3 ORBITAL PERIOD STUDY

We obtained new minimum times for FG Sct, VZ Lib and VZ Psc with help from the method developed by Kwee & van Woerden (1956) that implements a polynomial fitting program. Since the asymmetry of LCs affects the determination of minima, we calculated the minima by using the phase region ($\pm$0.04). Consequently, we obtained four new minimum times for FG Sct, five new minimum times for VZ Lib and seven new minimum times for VZ Psc (Table 2). In order to study the period variation and obtain updated ephemerides, we also collected all published minima in the literatures (Diethelm 2010; Qian et al. 2008; Ma et al. 2018; etc.) and the Eclipsing Binaries Minima Database (Paschke & Brat 2006). We also listed the results as well as minima types (Pri refers to primary, Sec refers to secondary) and observational methods (Pe: photoelectric, CCD: charge-coupled device, Pg: photograph) of these minima in Tables 3 and 4. Because of the differing measurement accuracies, we assigned weighting factors of

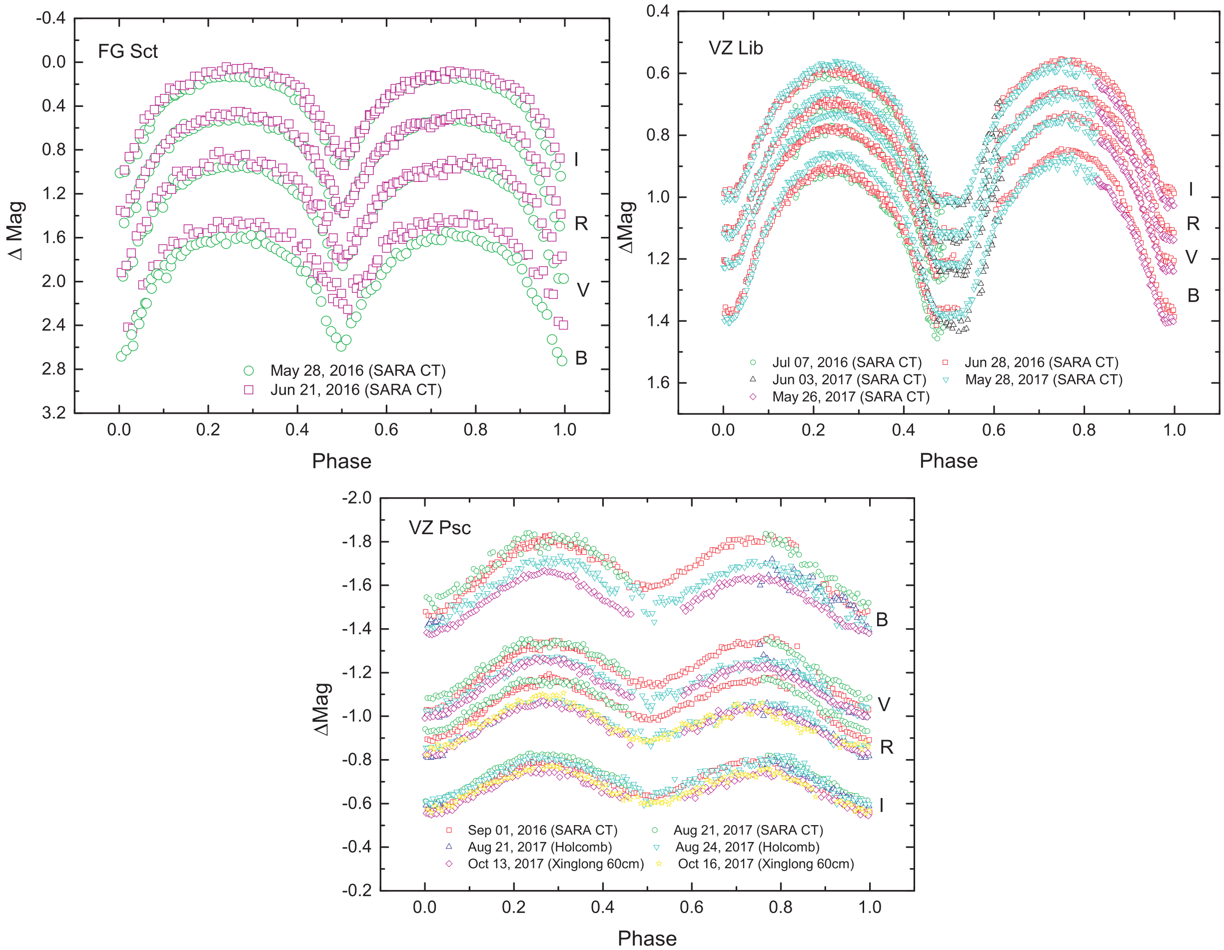

Fig. 1 B, V, R and I LCs for the three short-period eclipsing binaries in this work.

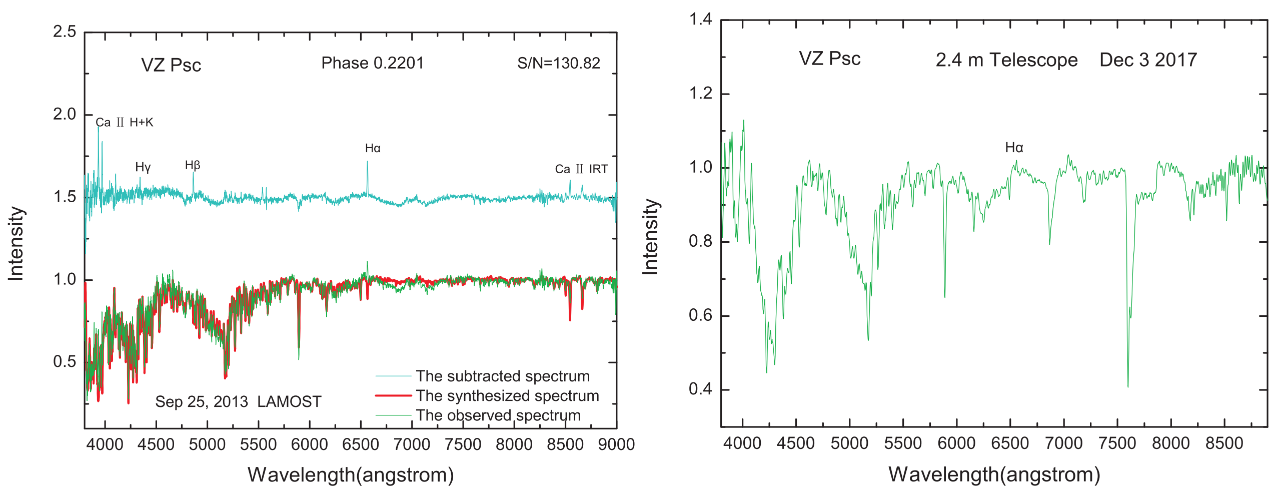

Fig. 2 Low-resolution spectra of VZ Psc observed by LAMOST on 2014 Apr 20 and the Lijiang 2.4-m telescope on 2017 Dec 3.

1 and 10 to visual and Pe/CCD data respectively. The mean errors of CCD minima are about 0.0010 d. The visual timings have a relatively large degree of uncertainty. The data dispersion of visual timing is about 0.01 d. The weight factors 1 for visual and 10 for CCD data have been used in the analysis of other eclipsing binaries (Yang et al. 2009; Yang & Liu 2003).

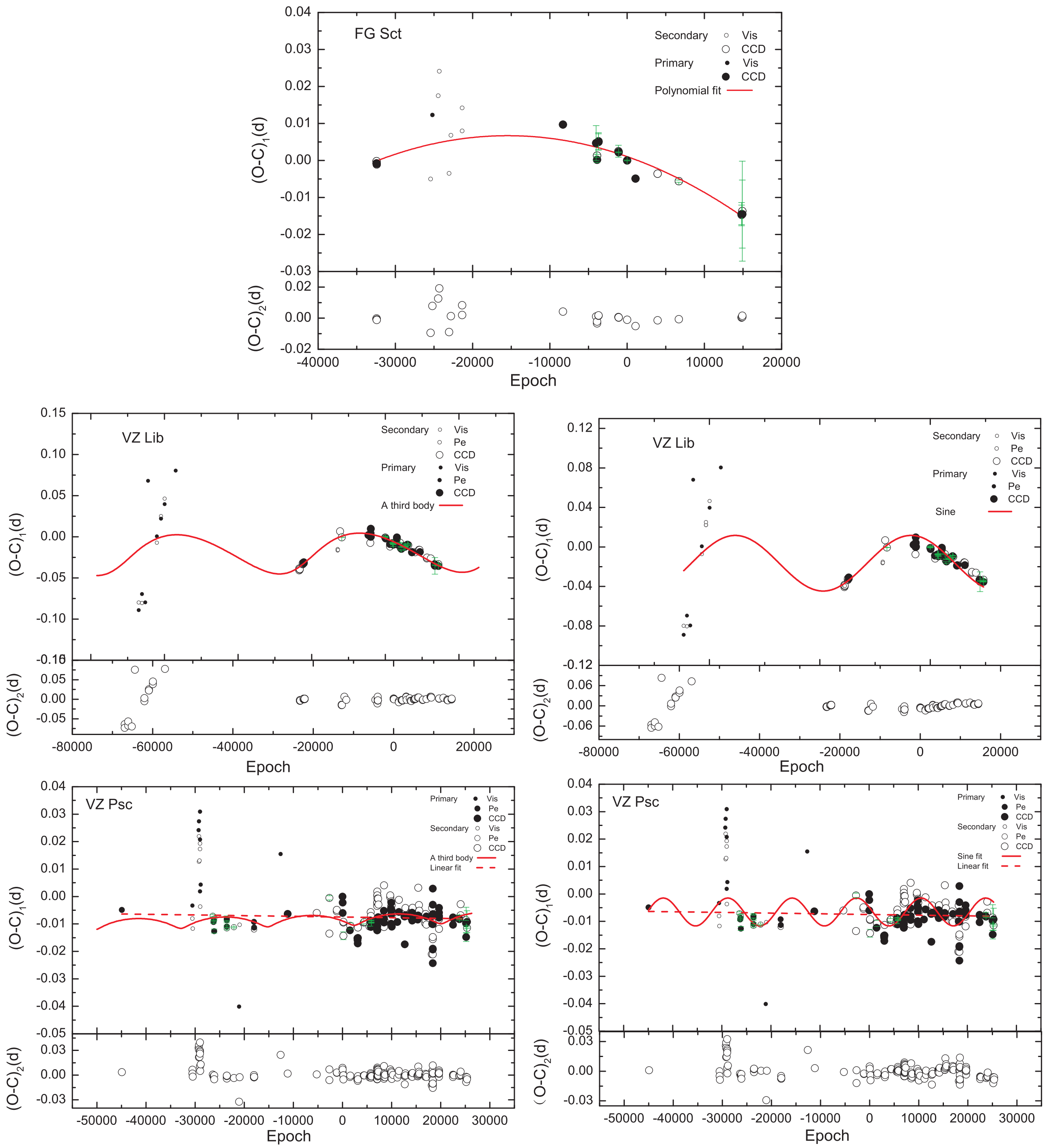

Fig. 3 $(O-C)$ diagrams for FG Sct, VZ Lib and VZ Psc. The $(O-C)_1$ values are calculated using a newly determined linear ephemeris (Eqs. (1), (3) and (6)). The *lines* represent different theoretical fits for the cyclic variation. Errors in some data are expressed by error bars.

3.1 Period Analysis of FG Sct

For FG Sct, we gathered 30 light minimum times, and listed them in Table 3. Combined with our newly obtained light minimum times, the linear ephemeris was updated

$$\begin{aligned}\mathrm{Min.I} = &\mathrm{HJD}2453528.9412(\pm0.0016)\\ &+0.27057199^{\mathrm{d}}(\pm0.0000001)\times E\,,\end{aligned}\tag{1}$$

where 2453528.9412 is the initial epoch, 0.27057199 d is the orbital period, E is the epoch number and the corre-

Table 3 Minimum Times and Relevant Parameters for FG Sct

System	HJD	Error	Min	Method	Cycle	$(O-C)_1$	$(O-C)_2$	Reference
	2444752.9378	-	Pri	Pg	–32435	–0.0009	–0.0005	[1]
	2444752.9376	-	Pri	CCD	–32435	–0.0011	–0.0007	[2]
	2444753.8852	-	Sec	CCD	–32431.5	–0.0005	–0.0001	[2]
	2444754.8315	-	Pri	CCD	–32428	–0.0012	–0.0008	[2]
	2444759.8368	-	Sec	CCD	–32409.5	–0.0014	–0.0011	[2]
	2446642.4730	-	Sec	Vis	–25451.5	–0.0051	–0.0093	[1]
	2446704.3160	-	Pri	Vis	–25223	0.0121	0.0078	[1]
	2446909.5500	-	Sec	Vis	–24464.5	0.0172	0.0126	[1]
	2446948.5190	-	Sec	Vis	–24320.5	0.0238	0.0191	[1]
	2447294.5530	-	Sec	Vis	–23041.5	–0.0036	–0.0088	[1]
	2447353.5480	-	Sec	Vis	–22823.5	0.0066	0.0013	[1]
	2447747.5020	-	Sec	Vis	–21367.5	0.0077	0.0020	[1]
	2447748.3200	-	Sec	Vis	–21364.5	0.0140	0.0083	[1]
FG Sct	2451277.7920	-	Pri	CCD	–8320	0.0097	0.0042	[1]
	2452440.4349	0.0047	Pri	CCD	–4023	0.0048	0.0011	[3]
	2452472.3579	0.0007	Pri	CCD	–3905	0.0003	–0.0033	[4]
	2452472.4943	0.0003	Sec	CCD	–3904.5	0.0014	–0.0022	[4]
	2452524.3125	0.0022	Pri	CCD	–3713	0.0050	0.0015	[3]
	2452524.3127	0.0023	Pri	CCD	–3713	0.0052	0.0017	[3]
	2453224.4151	0.0016	Sec	CCD	–1125.5	0.0026	0.0006	[5]
	2453228.3381	0.0001	Pri	CCD	–1111	0.0023	0.0004	[5]
	2453228.4735	0.0002	Sec	CCD	–1110.5	0.0024	0.0005	[5]
	2453528.9414	0.0001	Pri	CCD	0	0.0002	–0.0010	[6]
	2453823.8600	-	Pri	CCD	1090	–0.0046	–0.0050	[7]
	2454593.2328	-	Sec	CCD	3933.5	–0.0033	–0.0013	[8]
	2455340.8212	0.0003	Sec	CCD	6696.5	–0.0053	–0.0006	[7]
	2457536.7745	0.0026	Sec	CCD	14812.5	–0.0143	0.0003	[9]
	2457536.9099	0.0031	Pri	CCD	14813	–0.0141	0.0004	[9]
	2457560.7204	0.0092	Pri	CCD	14901	–0.0140	0.0007	[9]
	2457560.8565	0.0135	Sec	CCD	14901.5	–0.0132	0.0015	[9]

References: [1] Data from $O-C$ gateway (`http://var.astro.cz/ocgate/`); [2] Bradstreet (1985); [3] Zejda (2004); [4] Demircan et al. (2003); [5] Zejda et al. (2006a); [6] Krajci (2006); [7] Diethelm (2010); [8] Nagai (2009); [9] This paper.

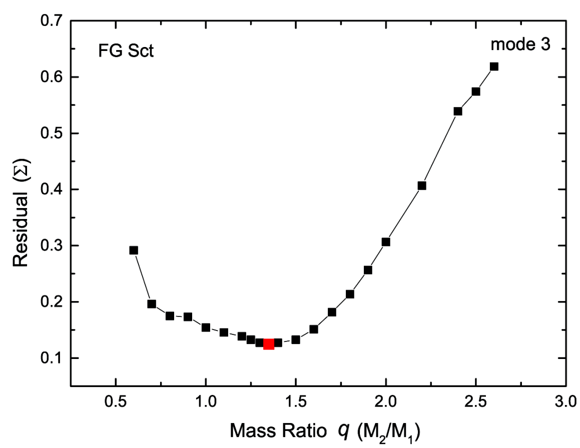

Fig. 4 Relationships between the residual sum of squares and the mass ratio q for FG Sct.

sponding deviations are given in parentheses. We calculated and obtained the fitting residual $(O-C)_1$ (residuals of linear fit) values and tabulated them in the seventh column of Table 3. Then we plotted $(O-C)_1$ versus epoch number E in Figure 3, which shows a downward parabolic trend. By analyzing these residuals, we obtained the fol-

Table 4 Minimum Times and Relevant Parameters of VZ Lib and VZ Psc

Object	HJD	Error	Min	Method	Cycle	$(O-C)_1$	$(O-C)_2$ (3rd body)	$(O-C)_2$ Sine	Reference
	2428731.3080	-	Sec	Vis	–66980.5	–0.0659	–0.0640	–0.0557	[1]
	2428731.4780	-	Pri	Vis	–66980	–0.0750	–0.0732	–0.0649	[1]
	2429046.2150	-	Sec	Vis	–66101.5	–0.0663	–0.0676	–0.0594	[1]
	2429046.4050	-	Pri	Vis	–66101	–0.0554	–0.0567	–0.0485	[1]
	2429369.1840	-	Pri	Vis	–65200	–0.0655	–0.0696	–0.0620	[1]
	2429645.0100	-	Pri	Vis	–64430	–0.0970	0.0757	0.0828	[2]
	2430493.2860	-	Sec	Vis	–62062.5	0.0067	–0.0049	–0.0009	[1]
	2430493.4730	-	Pri	Vis	–62062	0.0146	0.0029	0.0069	[1]
	2430899.2200	-	Pec	Vis	–60929.5	0.0361	0.0226	0.0246	[1]
	2430899.2230	-	Pec	Vis	–60929.5	0.0391	0.0256	0.0276	[1]
	2430899.3990	-	Pri	Vis	–60929	0.0360	0.0225	0.0245	[1]
	2431256.2400	-	Pri	Vis	–59933	0.0536	0.0388	0.0390	[1]
	2431256.4260	-	Sec	Vis	–59932.5	0.0604	0.0456	0.0458	[1]
	2432337.6780	-	Pri	Vis	–56914	–0.0846	0.0780	0.0725	[1]
	2432337.6780	-	Pri	Vis	–56914	–0.0846	0.0780	0.0725	[1]
	2444366.7339	-	Sec	CCD	–23337.5	–0.0271	–0.0041	–0.0037	[3]
VZ Lib	2444366.7353	-	Sec	Pe	–23337.5	–0.0257	–0.0027	–0.0023	[3]
	2444366.7359	-	Sec	CCD	–23337.5	–0.0251	–0.0021	–0.0017	[3]
	2444366.7362	-	Sec	CCD	–23337.5	–0.0248	–0.0018	–0.0014	[3]
	2444408.6509	-	Sec	CCD	–23220.5	–0.0261	–0.0035	–0.0030	[3]
	2444408.6512	-	Sec	Pe	–23220.5	–0.0258	–0.0032	–0.0027	[3]
	2444408.6514	-	Sec	CCD	–23220.5	–0.0256	–0.0030	–0.0025	[3]
	2444698.8448	-	Sec	CCD	–22410.5	–0.0199	–0.0000	0.0009	[3]
	2444698.8453	-	Sec	CCD	–22410.5	–0.0194	0.0004	0.0014	[3]
	2444698.8455	-	Sec	Pe	–22410.5	–0.0192	0.0006	0.0016	[3]
	2444698.8464	-	Sec	CCD	–22410.5	–0.0183	0.0015	0.0025	[3]
	2444787.5147	-	Pri	CCD	–22163	–0.0185	0.0004	0.0016	[3]
	2444787.5152	-	Pri	Pe	–22163	–0.0180	0.0009	0.0021	[3]
	2444787.5154	-	Pri	CCD	–22163	–0.0178	0.0011	0.0023	[3]
	2444787.5154	-	Pri	CCD	–22163	–0.0178	0.0011	0.0023	[3]
	2444788.5899	-	Pri	CCD	–22160	–0.0181	0.0008	0.0020	[3]
	2444788.5900	-	Pri	Pe	–22160	–0.0180	0.0009	0.0021	[3]
	...	...	...	...	...	...	...	...	...
	2439677.2520	-	Pri	Pe	–44931	0.0038	0.0037	0.0009	[30]
	2443431.2870	-	Pri	Vis	–30562	0.0052	0.0065	–0.0001	[1]
	2443432.4580	-	Sec	Vis	–30557.5	0.0006	0.0018	–0.0048	[1]
	2443446.3010	-	Sec	Vis	–30504.5	–0.0031	–0.0018	–0.0086	[1]
	2443764.4200	-	Pri	Vis	–29287	0.0327	0.0332	0.0258	[1]
	2443780.3600	-	Pri	Vis	–29226	0.0359	0.0363	0.0290	[1]
	2443780.4760	-	Sec	Vis	–29225.5	0.0213	0.0216	0.0143	[1]
	2443783.3590	-	Sec	Vis	–29214.5	0.0304	0.0308	0.0234	[1]
	2443812.3500	-	Sec	Vis	–29103.5	0.0217	0.0220	0.0146	[1]
	2443832.3440	-	Pri	Vis	–29027	0.0293	0.0296	0.0223	[1]
	2443835.2280	-	Pri	Vis	–29016	0.0395	0.0397	0.0324	[1]
	2443835.3470	-	Sec	Vis	–29015.5	0.0279	0.0281	0.0208	[1]
	2443836.2440	-	Pri	Vis	–29012	0.0105	0.0107	0.0034	[1]
	2443836.3900	-	Sec	Vis	–29011.5	0.0258	0.0261	0.0188	[1]
	2443842.3780	-	Sec	Vis	–28988.5	0.0049	0.0051	–0.0021	[1]
	2443876.2190	-	Pri	Vis	–28859	0.0128	0.0130	0.0058	[1]
	2444519.5585	0.0005	Sec	Pe	–26396.5	0.0015	0.0007	–0.0024	[31]
	2444556.5244	0.0005	Pri	Pe	–26255	–0.0007	–0.0015	–0.0044	[31]
VZ Psc	2444569.5880	0.0005	Pri	Pe	–26205	–0.0001	–0.0009	–0.0037	[31]
	2444588.5300	0.0007	Sec	Pe	–26132.5	0.0006	–0.0002	–0.0028	[31]
	2444591.5298	0.0007	Pri	Pe	–26121	–0.0040	–0.0048	–0.0074	[31]
	2445259.7046	0.0005	Sec	Pe	–23563.5	0.0002	–0.0007	0.0024	[31]
	2445260.6163	0.0005	Pri	Pe	–23560	–0.0024	–0.0034	–0.0002	[31]
	2445262.5751	0.0005	Sec	Pe	–23552.5	–0.0030	–0.0041	–0.0009	[31]

Table 4 — *Continued.*

Object	HJD	Error	Min	Method	Cycle	$(O-C)_1$	$(O-C)_2$ (3rd body)	$(O-C)_2$ Sine	Reference
	2445264.5375	0.0010	Pri	Pe	–23545	–0.0001	–0.0011	0.0020	[31]
	2445265.5831	0.0010	Pri	Pe	–23541	0.0004	–0.0006	0.0025	[31]
	2445639.3113	0.0002	Sec	Pe	–22110.5	–0.0026	–0.0035	0.0004	[32]
	2445915.5640	-	Pri	Vis	–21053	–0.0315	–0.0322	–0.0292	[1]
	2445939.4990	-	Sec	Vis	–20961.5	–0.0017	–0.0024	0.0004	[33]
	2446709.6894	-	Sec	Pe	–18013.5	–0.0035	–0.0027	–0.0076	[34]
	2446709.8228	-	Pri	Pe	–18013	–0.0007	0.0001	–0.0048	[34]
	2446710.7344	-	Sec	Pe	–18009.5	–0.0035	–0.0027	–0.0076	[34]
	2446710.8658	-	Pri	Pe	–18009.	–0.0027	–0.0020	–0.0069	[34]
	2448122.4760	-	Pri	Vis	–12606	0.0239	0.0245	0.0215	[1]
	2448500.2350	-	Pri	CCD	–11160.	0.0020	0.0018	0.0030	[1]
	2450042.3178	-	Sec	CCD	–5257.5	0.0023	0.0009	–0.0007	[35]
	...	...	...	...	...	...	...	...	...

References: [1] Data from the $O-C$ gateway (`http://var.astro.cz/ocgate/`); [2] Watson (2006); [3] Claria & Lapasset (1981); [4] Zejda et al. (2006a); [5] Szalai et al. (2007); [6] Perryman et al. (1997); [7] Lu et al. (2001); [8] Nagai (2008a); [9] Watanabe (2000); [10] Qian et al. (2008); [11] Zola et al. (2004); [12] Nagai (2004); [13] Krajci (2006); [14] Zejda et al. (2006b); [15] Ogloza et al. (2008); [16] Nagai (2007); [17] Diethelm (2011a); [18] Bonnardeau (2009); [19] Nagai (2009); [20] Samolyk (2009); [21] Marino et al. (2010); [22] Nagai (2011); [23] Diethelm (2012a); [24] Kazuo (2013); [25] Hoňková et al. (2013); [26] Nagai (2015); [27] Nagai (2016); [28] Nagai (2017); [29] This paper; [30] Eggen (1967); [31] Bradstreet (1985); [32] Poretti (1984); [33] Poretti (1985); [34] Samec & Bookmyer (1987); [35] Agerer & Hubscher (1996); [36] Agerer & Huebscher (1998); [37] Nagai (1999); [38] Nagai (2001); [39] Agerer & Hubscher (2002); [40] Nagai (2002); [41] Dvorak (2003); [42] Nagai (2003); [43] Qian et al. (2004); [44] Nelson (2004); [45] Senavci et al. (2007); [46] Nagai (2005); [47] Nagai (2006); [48] Dvorak (2006); [49] Diethelm (2006); [50] Hubscher & Walter (2007); [51] Nagai (2008b); [52] Hubscher et al. (2009); [53] Brat et al. (2011); [54] Nagai (2010); [55] Diethelm (2011b); [56] Nagai (2012); [57] Diethelm (2012b); [58] Hubscher (2013); [59] Diethelm (2013); [60] Honková et al. (2014); [61] Nagai (2014); [62] Hubscher (2017). All available data in this table are listed in the online version (`http://www.raa-journal.org/docs/Supp/Table4.dat`). Here lists partial contents to exhibit its form for reference.

Table 5 Parameters of the Assumed Third Body for Eclipsing Binary VZ Lib

Parameter	Value (VZ Lib)
A (d)	0.0249(±0.0004)
P_3 (yr)	48.69(±0.06)
e	0.258(±0.003)
T_0 (HJD)	2452727.5847(±0.0003)
$a_{12}\sin i$ (AU)	4.32(± 0.07)
$K_{\rm RV}$ (km s^{-1})	2.73(±0.07)
$f(m)$ $(M_\odot)$	0.034(±0.002)

lowing quadratic ephemeris

$$\begin{aligned}\text{Min.I} =& \text{HJD}2453528.9424(\pm 0.0001)\\ &+ 0.27057127^{\rm d}(\pm 0.00000002) \times E \\ &+ (-0.237)(\pm 0.009) \times 10^{-10} \times E^2\ .\end{aligned} \tag{2}$$

The residuals of the polynomial fit can be found in the eighth column of Table 3, which are named $(O-C)_2$. The quadratic term (–0.237×10^{-10}) indicates that the orbital period decreases at a speed of $6.39(\pm0.24)\times10^{-8}$ d yr^{-1}.

3.2 Period Analysis of VZ Lib

The 109 light minimum times we collected for VZ Lib are listed in Table 4. Through a least-squares fitting technique, we obtained an updated ephemeris

$$\begin{aligned}\text{HJD (Min.I)} =& \text{HJD}2452727.5714(\pm 0.0017)\\ &+ 0.35825647^{\rm d}(\pm 0.0000001) \times E\ ,\end{aligned} \tag{3}$$

where 2452727.5714 is the initial epoch, 0.35825647 d is the orbital period and E is the epoch number. We computed the fitting residual $(O-C)_1$ values and listed them in the seventh column of Table 4. The residuals $(O-C)_1$ reveal a potential cyclic orbital period variation (Fig. 3). This variation of the VZ Lib period might be caused by light time effect (LITE) via a tertiary component, which had been pointed out by Szalai et al. (2007) and Qian et al. (2008). Assuming the presence of a tertiary companion (Irwin 1952; Pribulla & Rucinski 2006; Yang et al. 2007),

Table 6 Photometric Solutions of the Three Eclipsing Binaries

Parameter	FG Sct	VZ Lib	VZ Lib	VZ Psc	VZ Psc
Reference	[1]	[1]	[2]	[1]	[3]
T_1 (K)	4536±140	5770±2	5770	4908±8	4500
a ($R_\odot$)	2.073144	2.357985	-	1.897763	-
M_1 ($M_\odot$)	0.694	0.998	1.06	0.742	0.651
M_2 ($M_\odot$)	0.9369	0.3708	0.35	0.5998	0.520
R_1 ($R_\odot$)	0.746	1.028	1.17	0.798	-
R_2 ($R_\odot$)	0.956	1.064	0.72	0.648	-
$q(M_2/M_1)$	1.35±0.001	0.37±0.002	0.33	0.81±0.002	0.8
i (°)	89.9±0.4	88.8±0.2	88.4	56.3±0.2	53.2
T_2 (K)	4373 ±112	5880±6	5980	4011±42	3949
$\Omega_{\rm in}$	4.2996	2.6163	-	3.4340	3.4170
$\Omega_{\rm out}$	3.7304	2.3891	-	2.9789	2.9666
$\Omega_1 = \Omega_2$	4.1775±0.0083	2.5286±0.0052	2.498	2.9982±0.0078	2.99201±0.0128
$L_1/(L_1+L_2)(B)$	0.5154±0.0021	0.6865±0.0005	-	0.8720±0.0016	0.4930±0.0277
$L_1/(L_1+L_2)(V)$	0.4988±0.0014	0.6920±0.0004	-	0.8286±0.0023	0.4601±0.0260
$L_1/(L_1+L_2)(R)$	0.4827±0.0011	0.6944±0.0003	-	0.7820±0.0030	0.4262±0.0241
$L_1/(L_1+L_2)(I)$	0.4724±0.0012	0.6960±0.0003	-	0.7347±0.0029	0.3657±0.0205
$L_3/(L_1+L_2)(B)$	-	0.0142±0.00003	-	0.0604±0.0006	-
$L_3/(L_1+L_2)(V)$	-	0.0155±0.00004	-	0.0782±0.0007	-
$L_3/(L_1+L_2)(R)$	-	0.0161±0.00004	-	0.0860±0.0007	-
$L_3/(L_1+L_2)(I)$	-	0.0186±0.00004	-	0.0865±0.0005	-
r_1 (pole)	0.3447±0.0009	0.4562±0.0011	-	0.4427±0.0015	0.4432±0.0024
r_1 (side)	0.3632±0.0012	0.4925±0.0015	-	0.4860±0.0022	0.4864±0.0036
r_1 (back)	0.4032±0.0018	0.5257±0.0021	-	0.5876±0.0060	0.5866±0.0093
r_1 (average)	0.3704±0.0013	0.4915±0.0016	-	0.5054±0.0032	-
r_2 (pole)	0.3945±0.0009	0.2950±0.0015	-	0.4089±0.0015	0.4070±0.0025
r_2 (side)	0.4187±0.0012	0.3104±0.0019	-	0.4469±0.0022	0.4443±0.0036
r_2 (back)	0.4550±0.0017	0.3593±0.0039	-	0.5922±0.0131	0.5842±0.0185
r_2 (average)	0.4227±0.0013	0.3216±0.0024	-	0.4827±0.0056	-
f (%)	21.4±0.04	38.6±0.08	19.4	95.7±0.25	94.4±2.8
RSS	0.1245	0.2125	-	2.5063	-

References: [1] This study; [2] Szalai et al. (2007); [3] Ma et al. (2018).

we fitted the $(O-C)_1$ values, yielding

$$(O-C)_1 = \frac{a_{12}\sin i}{c} \times \left[\frac{1-e^2}{1+e\cos v}\sin(v+\omega) + e\sin\omega\right] . \tag{4}$$

In Equation (4), $a_{12}\sin i/c$ stands for the semi-amplitude of LITE, a_{12} is the semi-major axis of the eclipsing-pair orbiting the centroid with the tertiary component, c is the light speed, i is the inclination, e is eccentricity, v is true anomaly and ω represents longitude of the periastron (Irwin 1952). In order to derive parameters from the equation above, the Levenberg-Marquardt method was applied (Yang et al. 2011; Press et al. 1992). The determined parameters are given in Table 5. We also provided the fitting residual $(O-C)_2$ values in the eighth column of Table 4. From these parameters, we obtained the orbital period of the tertiary component as $48.7(\pm0.1)$ yr.

LITE due to the existence of a tertiary component is not the only possible cause for cyclic orbital period variation. Magnetic activity could also give rise to cyclic period changes. This mechanism hypothesizes that a hydromagnetic dynamo could affect the gravitational quadrupole moment of the active component (Lanza & Rodonò 2002). If we think that it causes a sinusoidal variation in the orbital period, we could obtain

$$\begin{aligned}(O-C)_1 = &-0.017(\pm0.003) + 0.028^{\rm d}(\pm0.003)\\ &\times \sin[0.000132(\pm0.000006)\,({\rm rad}^{-1})\\ &\times E - 4.024195\,({\rm rad})] .\end{aligned} \tag{5}$$

From the above equation, the amplitude of the cyclic oscillation is $0.028(\pm0.003)$ d. Making use of equation $T = 2\pi \times P/\omega$, in which P denotes the orbital period and ω refers to the coefficient of E, we derived the oscillation period T, which is $46.9(\pm1.9)$ yr. The $(O-C)_2$ values of the fitting residuals are listed in Table 4. Qian et al. (2008) fitted the $O-C$ diagram with a sinusoidal function and reported a period of 17.1 yr for the cyclic oscillation. Bonnardeau (2009) fitted the $O-C$ diagram with LITE and reported the period of 34.8 yr. The periods obtained by us were larger than the previous results (Qian et al. 2008; Bonnardeau 2009).

For the purpose of determining the source of differences between our results and previous studies (Qian et al. 2008; Bonnardeau 2009), we computed the time scales of all light minimum times. The time scales of all light minimum times in the study of Qian et al. (2008) are from epochs –64430.5 to 4010.5 and the time scale of Bonnardeau (2009) is from epochs –64430.5 to 6263.5. The time scales of light minimum times adopted by us vary from –66980.5 to 14459.5 epochs. As can be seen from Figure 3, the curve is also deceasing from epochs 6263.5 to 14459.5. The longer time scale of minimum times implies that the period of the potential oscillation is larger than the previous results (Qian et al. 2008; Bonnardeau 2009).

To quantitatively evaluate our goodness of fit and compare with previously published work, we calculated the Akaike information criterion (AIC) values (Akaike 1974) based on the same light minimum times. Supposing that the model's residuals independently obey a normal distribution, then AIC values can be derived based on AIC= $2k + n\ln$(RSS), in which k is number of parameters, n is sample size and RSS is the residual sum of squares (Akaike 1974; Burnham & Anderson 2002). The smaller value of AIC indicates higher likelihood of correctness and only differences in AIC are meaningful. There are five parameters in both our fit with the LITE and in the fit of Qian et al. (2008). Qian et al. (2008) collected 21 light minimum times. The corresponding RSS values are 0.00018 and 0.00015 for the fits by us and Qian et al. (2008). Thus, the AIC value is –171.2 for our result of the fit with the LITE and the value is –174.7 for the previous fit by Qian et al. (2008). Our fit result is similar to that by Qian et al. (2008).

We calculated –323.6 for the AIC value of the fit with the LITE and –332.6 for the AIC value of the sinusoidal fit with magnetic activity in our study. Statistically, the model of magnetic activity is better than that of the third body. Since there are big discrepancies in the period for the cyclic oscillation of VZ Lib between our study and the previous work, more studies are needed to clarify this issue.

3.3 Period Analysis of VZ Psc

We collected 178 light minimum times of VZ Psc and listed them in Table 4. With the help of a least-squares fitting approach, we updated the ephemeris

$$\begin{aligned}\mathrm{HJD(Min.I)} =& \mathrm{HJD}2451415.8857(\pm0.0007)\\ &+ 0.26125921^{\mathrm{d}}(\pm0.00000004)\times E\,,\end{aligned} \tag{6}$$

where 2451415.8857 is the initial epoch, 0.26125921 d is the orbital period and E is epoch number. We listed the residuals of linear fit $(O-C)_1$ in the seventh column of Table 4 and plotted them in Figure 3. Qian et al. (2004) and Ma et al. (2018) found that there might be a cyclic variation in the $O-C$ data of VZ Psc. We also fitted the $O-C$ values using the linear function, LITE and magnetic activity cycle. The AIC values are –777.2 for the linear fit, –760.8 for the fit with LITE and –807.3 for the fit with magnetic activity cycle. However, there is a very weak cyclic variation because of similar AIC values from the $O-C$ fit using the three types of the fits. Therefore it is too early to assign statistical significance in the $O-C$ linear fitting residuals for VZ Psc.

4 PHOTOMETRIC ANALYSIS AND SPECTRAL ANALYSIS

Because our LCs for all three binary systems had full phase coverage, we acquired the photometric solution using the updated Wilson-Devinney (W-D) program (Wilson & Devinney 1971; Wilson 1979, 1990, 1994). Assuming that all three binaries, FG Sct, VZ Lib and VZ Psc, are contact binaries, we selected mode 3 (contact binary) in the code to try to find converged solutions for their model parameters.

We determined the effective temperature of the primary star (T_1) based on the relationship of the $J-H$ color index by Collier Cameron et al. (2007).

$$\begin{aligned}T_{\mathrm{eff}} =& -4369.5(J-H)\\ &+ 7188.2, 4000\,\mathrm{K} < T_{\mathrm{eff}} < 7000\,\mathrm{K}\,.\end{aligned} \tag{7}$$

We obtained J and H magnitude values by the 2MASS All Sky Catalog (Skrutskie et al. 2006). The J and H magnitudes are not usually obtained during the secondary eclipse of a totally eclipsing binary. The temperature from the color index is the total effective temperature of the system in some orbital phase, and not the temperature of the primary component. Therefore, we only used it as an initial value for the two components in the eclipsing binary and adjusted the separate temperatures from the LC fit to get more reliable values.

For FG Sct, Equation (7) gave the initial temperature of the primary star to be 4536 K. We employed our LC data from the 2016 May 28 observation. The other values in the W-D program are set as below: The bolometric albedo is

0.5 (Ruciński 1969) and gravity-darkening coefficients are 0.32 (Lucy 1967). The bolometric limb-darkening coefficients $X_{\rm bolo}$ and limb-darkening coefficients for $BVRI$ bands are $X_{1\rm bolo} = 0.533$, $X_{2\rm bolo} = 0.505$; $X_{1B} = 0.939$, $X_{2B} = 0.940$, $X_{1V} = 0.790$, $X_{2V} = 0.794$, $X_{1R} = 0.654$, $X_{2R} = 0.666$, $X_{1I} = 0.529$, $X_{2I} = 0.532$, respectively. Due to the lack of spectroscopic mass ratios for FG Sct, we tried different mass ratios q from 0.6 to 2.6 in the W-D program.

In Figure 4, we plotted the fitting residuals $\sum$ versus q and the smallest residual occurred at 1.35, which we applied in the final fitting. We adjusted all the orbital parameters and found they all converged simultaneously. The final theoretical and observed LCs of FG Sct are plotted in Figure 5. The orbital parameters and their errors are listed in Table 6. The formal errors given by the minimization algorithm for the fitting with the W-D code are not the true uncertainties of the model parameters (Prša & Zwitter 2005). More advanced statistical modeling would be required to derive the true uncertainties, therefore our model results should be understood as only crude estimates of the true parameters.

For VZ Lib, we modeled the photometric LC using data from observations on 2017 May 26 and 2017 May 28. We set the initial temperature for the primary component at 5973 K based on Equation (7). We fixed the bolometric albedo as 0.5 and gravity-darkening coefficients as 0.32. The bolometric limb-darkening coefficients $X_{\rm bolo}$ and limb-darkening coefficients for B, V, R and I bands are $X_{1\rm bolo} = 0.500$, $X_{2\rm bolo} = 0.520$; $X_{1B} = 0.709$, $X_{2B} = 0.781$, $X_{1V} = 0.579$, $X_{2V} = 0.644$, $X_{1R} = 0.478$, $X_{2R} = 0.533$, $X_{1I} = 0.392$, $X_{2I} = 0.438$, respectively. First, we assumed the temperature of the secondary component was less than that of the primary component. However, the W-D program could not produce theoretical LCs that fit the observed data well. Therefore, we assumed the secondary temperature is greater than that of the primary. Furthermore, a cool spot was needed on the primary component, in order to give an explanation for the phenomenon that Max.I (phase 0.25) was brighter than Max.II (phase 0.75). Radial velocities obtained by Lu et al. (2001) were used in the W-D program to determine a more accurate mass ratio. However, Lu et al. (2001) said in their paper that their radial velocity solution was relatively poor, so our theoretical fit to the radial velocities of VZ Lib is likely not good (Fig. 6). By contrast, photometric solutions obtained by Szalai et al. (2007) are listed in the fourth column of Table 6.

Similarly, for VZ Psc, we made use of data acquired on 2017 Aug 24 by the Holcomb Observatory. We assumed the initial temperature of the primary component as 4671 K based on Equation (7). The other parameters are as follows: The bolometric albedo $A_1 = A_2 = 0.5$ and gravity-darkening coefficients $g_1 = g_2 = 0.32$. The bolometric limb-darkening coefficients $X_{\rm bolo}$ and limb-darkening coefficients for B, V, R and I bands are $X_{1\rm bolo} = 0.536$, $X_{2\rm bolo} = 0.505$; $X_{1B} = 0.918$, $X_{2B} = 0.940$, $X_{1V} = 0.773$, $X_{2V} = 0.794$, $X_{1R} = 0.638$, $X_{2R} = 0.666$, $X_{1I} = 0.518$, $X_{2I} = 0.532$, respectively. When adjusting the W-D program, we simultaneously analyzed the radial velocities published by Hrivnak et al. (1995) to find a mass ratio, which is shown in Figure 6.

For VZ Psc, we also tried the LC modeling beginning with mode 2 (detached system) of the WD code. The RSS of the detached converged solution was 2.59, while the RSS of the contact solution was 2.51. For this reason, we chose the contact model as the more likely one for VZ Psc. For the detached model, the dimensionless potentials of primary and secondary components were between $\Omega_{\rm in}$ and $\Omega_{\rm out}$ for the corresponding mass ratio, which indicated that VZ Psc might not be a detached but rather a contact binary. We added a cool spot on the primary star to interpret the unequal heights of the two maxima. The spot parameters are listed in Table 7 and there are also small variations in starspot parameters. By contrast, photometric solutions obtained by Ma et al. (2018) are provided in the sixth column of Table 6. Our results (orbital inclination, temperatures of the two components and potentials) are similar to the previous results (Ma et al. 2018).

A high level of magnetic activity was believed to exist in VZ Psc (Wolff et al. 1965). To test this hypothesis, we analyzed its spectrum from the LAMOST survey to investigate chromospheric activity (Zhang et al. 2017). We analyzed its normalized spectrum using the spectral subtraction method by the program STARMOD (Barden 1985; Montes et al. 1995). The synthesized spectrum was created from the artificially rotationally broadened, radial-velocity shifted spectrum of an inactive star that is consistent with VZ Psc in spectral type and luminosity class. BD 22719 was used to create the template. The subtracted spectrum was created from the observed spectrum subtracting the synthesized spectrum. We present the synthesized and subtracted spectra in Figure 2. The subtracted one displays strong emissions in Ca II H&K, Hα, Hβ, Hγ and Ca II IRT lines. The equivalent widths (EWs) of the excess emissions were determined. The EWs and corresponding uncertainties are derived as follows: 1.852($\pm$0.001) Å and 2.802($\pm$0.169) Å for Ca II H&K; 2.227($\pm$0.016) Å for Hα; 1.205($\pm$0.079) Å for Hβ; 0.798($\pm$0.007) Å for Hγ; 0.210($\pm$0.014) Å, 1.257($\pm$0.018) Å and 1.159($\pm$0.004) Å

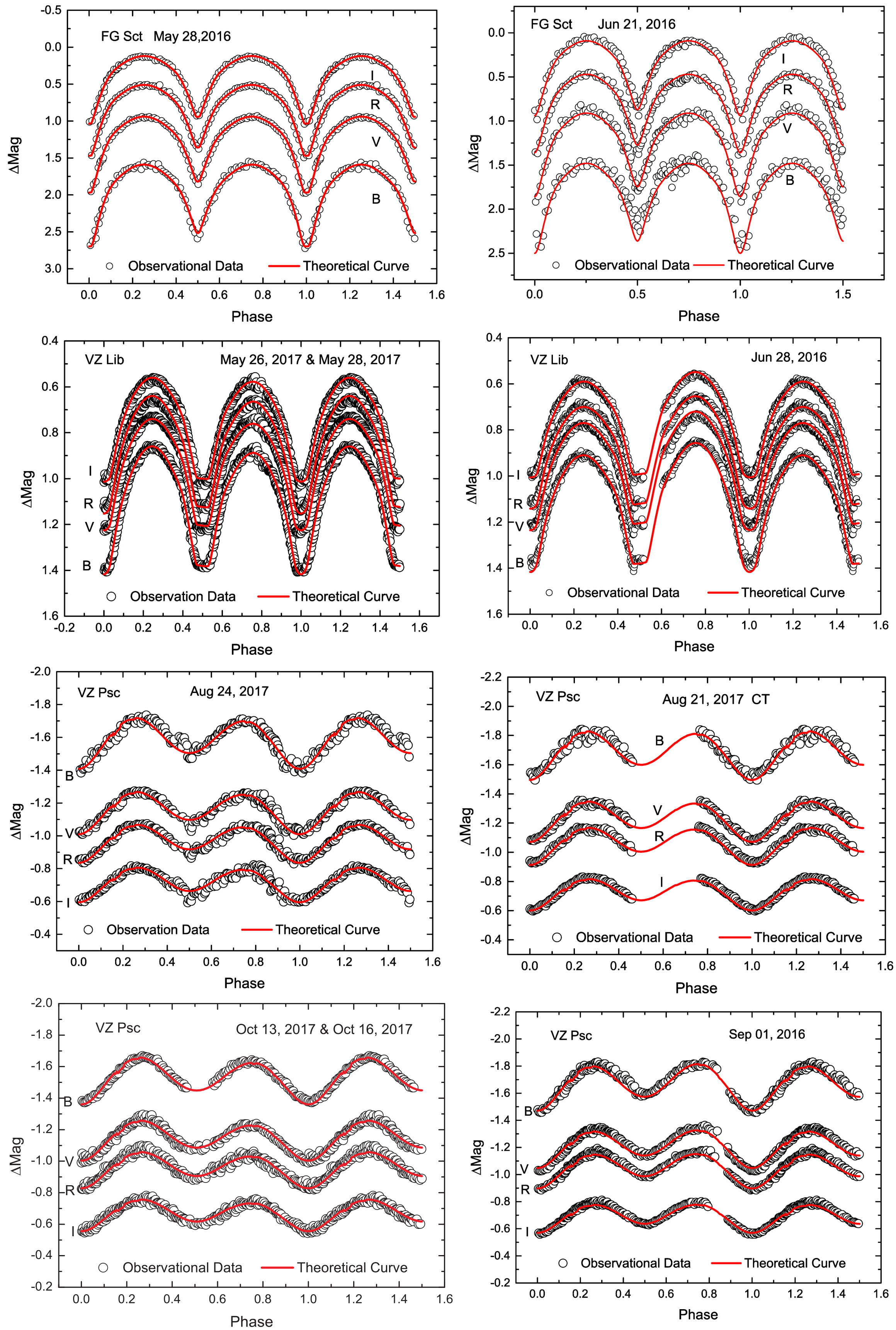

Fig. 5 Observed and theoretical LCs of the three short-period eclipsing binaries.

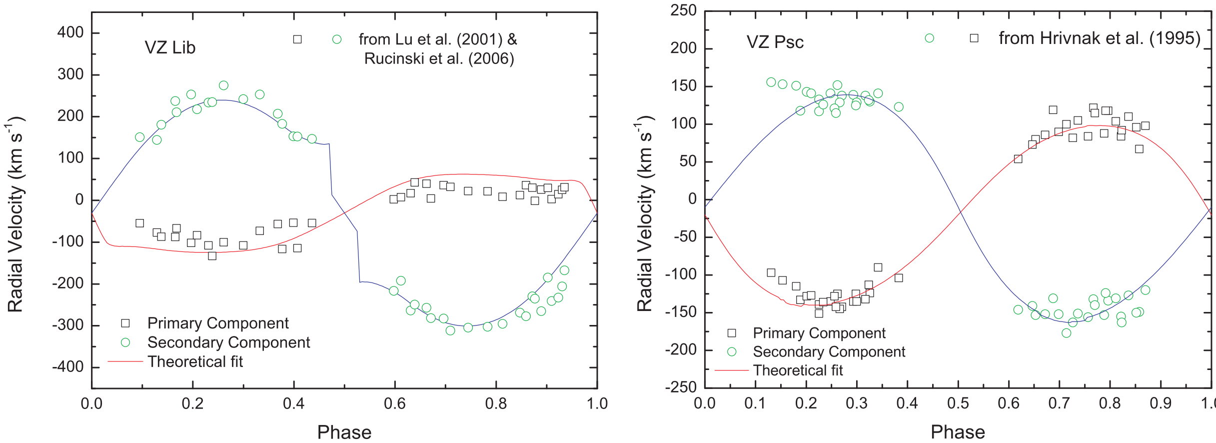

Fig. 6 The radial velocities of the primary and secondary components, and their fits for VZ Lib and VZ Psc.

Table 7 Spot Parameters of the Eclipsing Binaries VZ Lib and VZ Psc

Star	HJD	Spot Location	Colatitude	Longitude	Radius	T (K)	Reference
VZ Lib	2457899.69732	P	90°a	264.2°±0.1°	11.5°±0.3°	4405±77	[1]
	2457567.62160	P	90°a	91.6°±0.1°	15.3°±0.2°	3485±128	[1]
VZ Psc	2457989.76863	P	90°a	269.9°±0.5°	11.4°±0.3°	3606±442	[1]
	2457986.83618	P	90°a	269.9°±1.3°	11.4°±0.5°	4167±228	[1]
	2458040.23045	P	90°a	252.2°±1.3°	15.1°±0.5°	3167±333	[1]
	2457632.72418	P	90°a	259.4°±0.6°	11.5°±1.1°	5971±46	[1]
	2456897.10509	P	87°a	272.8°	35.2°	4776	[2]

Notes: Parameters not adjusted in the solution are denoted by symbol (a). P-Primary, S-Secondary. References: [1] This study; [2] Ma et al. (2018).

for Ca II IRT. Due to the low-resolution (about 1800) nature of this LAMOST spectrum, the spectral lines of the primary and secondary components were mixed. As a result, we had no way to ascertain the activity levels for each component of VZ Psc. For the spectrum obtained by the Lijiang 2.4-m telescope, administered by Yunnan Observatories, we processed with standard procedures (including image trimming, bias substraction, flat-field division, background substraction, cosmic ray removal and spectrum extraction). We acquired the wavelength calibration through the spectra of a Th-Ar lamp. Finally, the normalized spectra were derived by a polynomial fit to the observed continuum, which is displayed in Figure 2. We determined the chromospheric EW of the Hα line as 0.6282($\pm$0.0494). The spectral type was determined as K5 by means of Hammer spectral typing facility (West et al. 2004; Covey et al. 2007), with deviation of spectral type estimated at about two subtypes (West et al. 2004; Yi et al. 2014).

We adjusted the orbital and starspot parameters to obtain the final results. Details about the procedure can be found in the works of Zhang & Gu (2007) and Zhang et al. (2014) with regard to several eclipsing binaries. Because it was not easy to get the starspot latitude for VZ Lib and VZ Psc via photometry, we assumed starspots were located on their equators (starspot latitude is 90°). As a result, we only separately adjusted other starspot parameters until the theoretical LCs fitted the observed ones well. The resulting model parameters of the three binaries are listed in Table 6. The corresponding starspot parameters are available in Table 7. The three-dimensional grid models of Roche geometry are plotted in Figure 7. As can be seen from LCs and starspot parameters, there are long-term variations in VZ Psc and VZ Lib. In Figure 8, we plotted $\log(T_{\rm eff})$ vs. $\log(L/L_{\odot})$ for the primary and secondary components of this three binaries, which imply the primary components of these three binaries are all main sequence stars.

5 DISCUSSION AND CONCLUSIONS

In this section, we will estimate the physical parameters of the stars in these binaries and analyze the mechanisms (mass transfer between components, third bodies or magnetic braking) of orbital period variation.

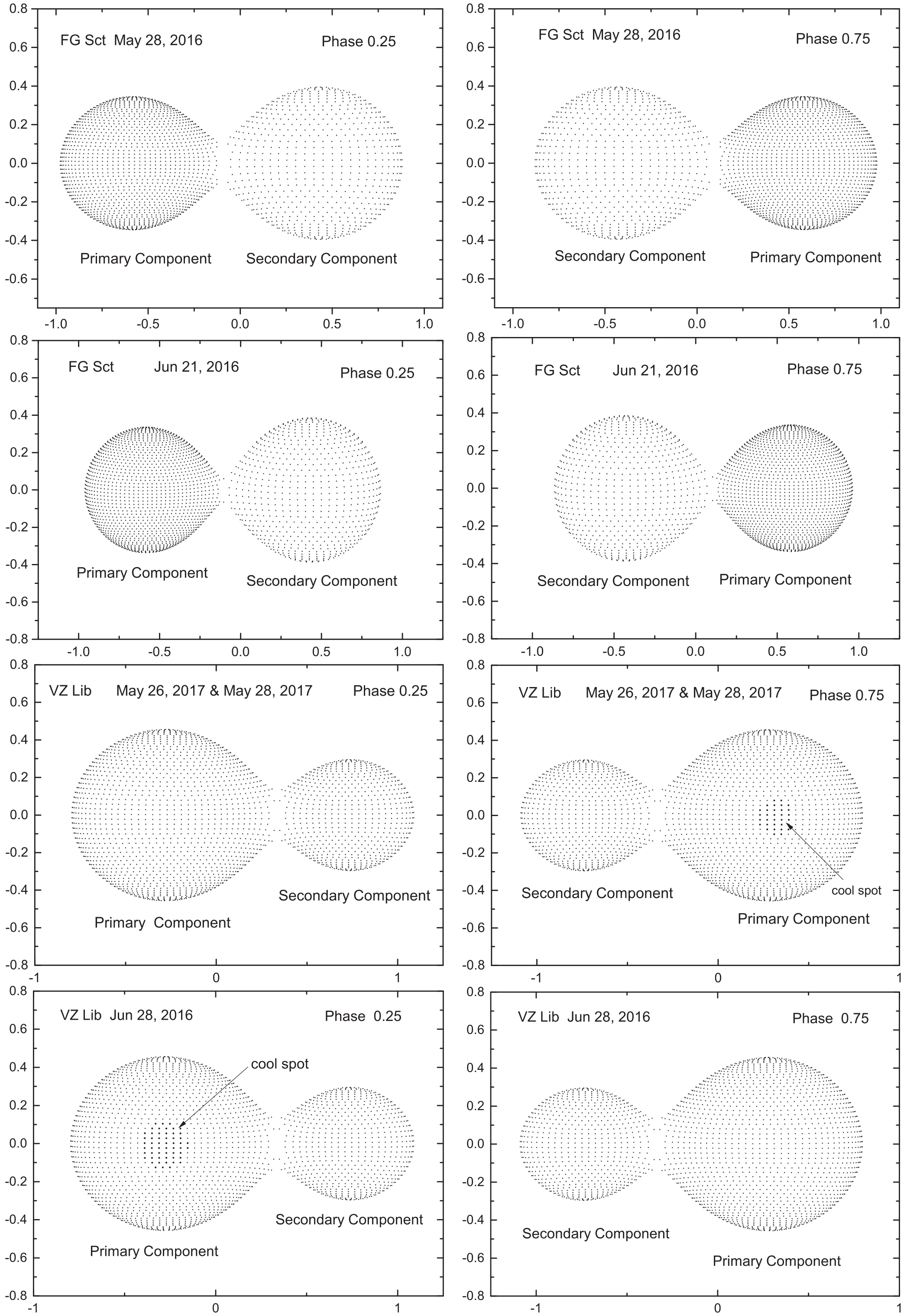

Fig. 7 Configurations and spot distributions of the three short-period eclipsing binaries.

5.1 FG Sct

For FG Sct, through analyzing its LC minimum times, we obtained the decreasing rate of its period as $-6.39(\pm0.24) \times 10^{-8}\,\mathrm{d\,yr^{-1}}$. Because of the mass ratio of 1.35, we firstly analyzed the relevant parameters for this period variation based on mass transfer from the secondary component to the primary component. We also analyzed this phenomenon by magnetic braking (Applegate 1992;

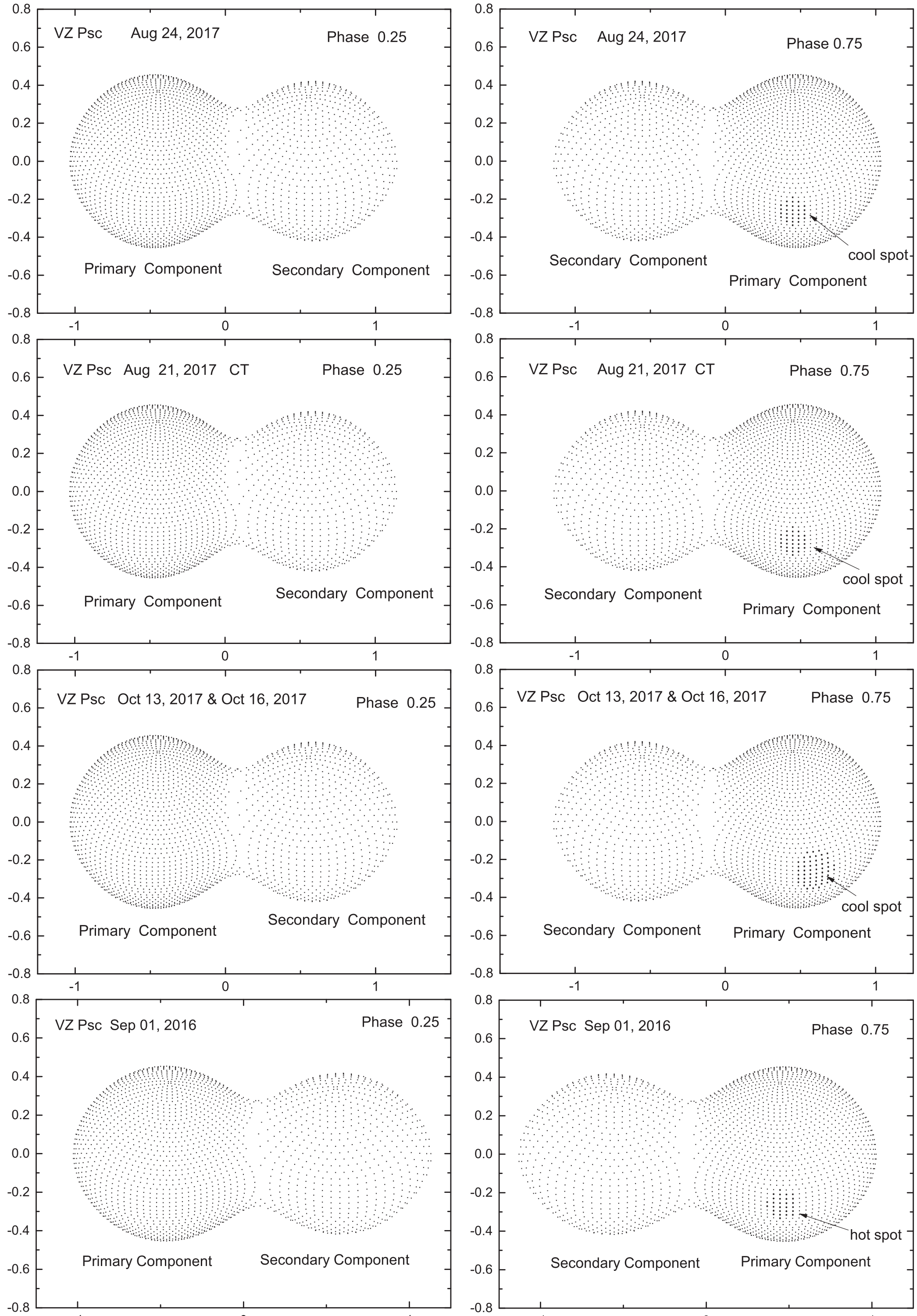

Fig. 7 —*Continued.*

Lanza et al. 1998; Hoffman et al. 2006). Using the equation below, the mass transfer rate could be computed (Singh & Chaubey 1986)

$$\frac{\dot{P}}{P} = 3\left(\frac{M_2}{M_1} - 1\right)\frac{\dot{M}_2}{M_2} \ . \tag{8}$$

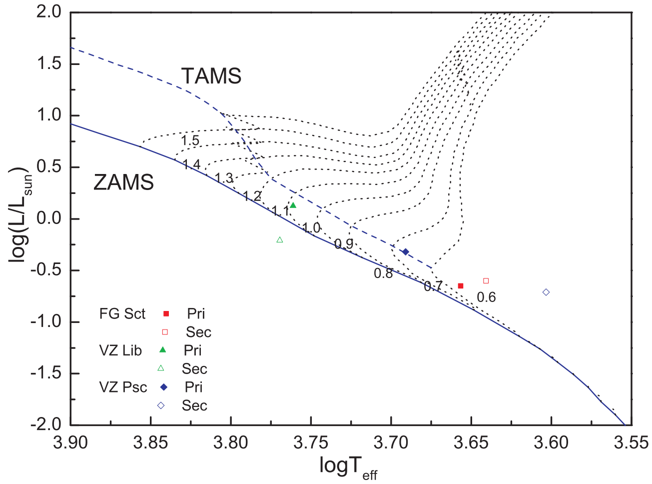

Fig. 8 $\log(T_{\rm eff}) - \log(L/L_\odot)$ diagram for the primary and secondary components of these three binaries.

Table 8 Contact Eclipsing Binaries with a Third Body, Similar to VZ Lib

Star name	M_1 ($M_\odot$)	M_2 ($M_\odot$)	Period (d)	f	T_1 (K)	T_2 (K)	q	$dp/dt(10^{-8})$	P_3 (yr)	A (d)	$f(m)$ ($M_\odot$)	Reference
AH Tauri	1.04	0.53	0.3326724	6.9%	5660	5633	0.50	–18.23	54.6	0.0349	0.0830	[1]
KIC002856960	0.22	0.24	0.2585079	-	3160	3067	1.11	-	205.2	-	0.2950	[2]
GN Boo	0.84	0.27	0.3016022	5.8%	6250	6879	0.32	-	9.9	0.0042	0.0040	[3]
V1918 Cyg	1.52	0.40	0.4131769	49.1%	7060	6924	0.26	–43.1	27.6	0.013	0.0150	[3]
SS Ari	1.30	0.40	0.4059862	9.4%	5860	5488	3.25	–40.3	37.8	0.0112	0.4075	[4]
TY Boo	1.08	0.55	0.3171478	7.6%	5108	5712	2.15	–3.65	58.9	0.0254	0.0263	[5]
DD Aqr	1.63	0.47	0.7210109	-	7550	4515	0.29	-	20.1	0.0034	0.0009	[6]
RR Lep	2.53	0.73	0.9154282	-	9300	4904	0.29	-	13.4	0.003	0.0009	[6]
LU Lac	0.80	0.38	0.2988019	8.9%	5310	4899	2.09	-	51.9	0.0125	0.0038	[7]
BX Peg	1.02	0.38	0.2804220	14.6%	5872	5300	2.66	–20.7	57.8	0.0152	0.0055	[8]
V728 Her	1.80	0.28	0.4712889	81.0%	6600	6743	0.16	19.2	-	0.02	0.0100	[9]
AB And	0.58	1.03	0:3318911	25.2%	5450	5020	1.79	14.6	98.3	0.121	0.0095	[10]
BO Ari	-	-	0.3181933	27.7%	6250	6409	0.18	–34.9	5.5	-	-	[11]
V776 Cas	1.60	0.21	0.4404140	79.0%	7910	5614	0.14	-	8.3	0.0013	-	[12]
UY UMa	1.19	0.16	0.3760192	5.0%	-	-	-	25.45	14.3	0.0026	0.0005	[13]
DY CVn	0.54	0.67	0.2459495	13.2%	4410	4297	1.25	-	-	-	-	[14]
V482 Per	1.51	1.29	-	-	6700	6340	0.86	-	16.6	0.018	0.3900	[15]

References: [1] Xiang et al. (2015); [2] Lee et al. (2013); [3] Yang et al. (2013); [4] Liu et al. (2009); [5] Christopoulou et al. (2012); [6] Erdem & Öztürk (2016); [7] Liao et al. (2014); [8] Li et al. (2015); [9] Erkan & Ulaş (2016); [10] Li et al. (2014); [11] Kriwattanawong et al. (2016); [12] Noori & Abedi (2017); [13] Yu et al. (2017); [14] Qu et al. (2017); [15] Baştürk et al. (2015).

We obtained the mass of the primary star (M_1) as 0.694 $M_\odot$ by the relationship between the star mass and color index (Cox 2000). Moreover, with a mass ratio of 1.35, we could determine the mass of the secondary star M_2 to be 0.9369 $M_\odot$. Finally, Equation (8) gave the mass transfer rate to be $\dot{M}_2$ =2.109($\pm$0.081)$\times 10^{-7} M_\odot$ yr^{-1}. By analyzing the photometric data, we obtained orbital parameters for FG Sct: the orbital inclination is 89.9° and the temperature of the secondary star T_2 is 4373 K, which is nearly 163 K less than that of the primary star. The fractions of the primary component luminosity to the total luminosity are 0.5154 for B band, 0.4988 for V band, 0.4827 for R band and 0.4724 for I band. The dimensionless potentials of two components are 4.178($\pm$0.007). On the basis of the above values, we had the ability to calculate the fillout factor between its two components by means of $f = (\Omega_{\rm in} - \Omega)/(\Omega_{\rm in} - \Omega_{\rm out})$. The result we obtained is $f(\%) = 21.4(\pm 0.04)$. In conclusion, FG Sct is a short-period eclipsing binary with a low degree of contact. Its decreasing orbital period implies mass transfer or magnetic braking.

5.2 VZ Lib

For VZ Lib, based on the relationship between the star mass and color index, we obtained the mass of primary

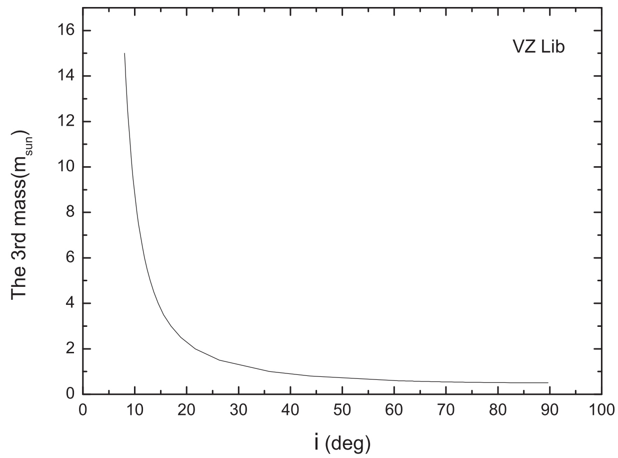

Fig. 9 Relationships between the mass of a tertiary component and the orbital inclination for VZ Lib.

component M_1 that is $0.998\,M_\odot$ (spectral type: G2). Owing to the mass ratio 0.37, the mass of the secondary M_2 is $0.3708\,M_\odot$. The fractions of the primary star luminosity to the total luminosity are 0.6865 for B band, 0.6920 for V band, 0.6944 for R band and 0.6960 for I band. The orbital inclination is $88.8°$. The dimensionless potential is $\Omega_1 = \Omega_2 = 2.5286(\pm 0.005)$. Lastly, the fill-out factor $f(\%)$ is 38.6($\pm$0.08). The $(O-C)$ diagram of VZ Lib shows a cyclic oscillation which may result from the effect of a tertiary component or magnetic activity cycles (sine). We firstly analyzed this cyclic period oscillation based on the LITE due to a tertiary companion. A tertiary component could play a vital role in its development by diminishing the angular momentum of the central binary. The semi-amplitudes $K_{\rm RV}$ of the changes in the systemic velocity were studied by Mayer (1990)

$$K_{\rm RV} = \frac{2\pi}{P_3}\frac{a_{12}\sin i}{\sqrt{1-e^2}}\,. \tag{9}$$

In the above equation, the units of $K_{\rm RV}$, a_{12} and P_3 are kilometers per second, kilometers and seconds respectively. From Equation (4) and the equation above, the semi-amplitudes for the tertiary component could be determined to be 2.734$\pm$0.0747 km s^{-1}. The mass function for the tertiary body (0.034$\pm$0.002 $M_\odot$) in Table 5 is obtained using the following formula

$$\begin{aligned} f(m) =& \frac{4\pi^2}{GT^2} \times (a'_{12}\sin i')^3 \\ =& \frac{(M_3 \sin i'_3)^3}{(M_1+M_2+M_3)^2}\,. \end{aligned} \tag{10}$$

The mass of the tertiary component also depends on orbital inclination i'. The relationship between the orbital inclination and the mass of the tertiary light is plotted in Figure 9. The minimum possible mass is 0.4897 $M_\odot$ for the tertiary body when the orbital inclination i is equal to $90°$. Through Allen's Astrophysical Quantities (Cox 2000), we know the spectral type of the tertiary light to be M0–M1.

The period oscillation in VZ Lib can also be caused by magnetic activity cycles. In terms of the formula $\Delta Q = -(\Delta p/p) \times (Ma^2/9)$ (Applegate 1992), we were able to calculate the change in the quadrupole moment $\Delta Q_{1,2}$ for primary and secondary components. Hypothesizing that the primary component of VZ Lib is a main-sequence G2 star, we could determine its radius as R_1=1.028 $R_\odot$ (Cox 2000), then the semimajor axis of this system is derived to be 2.357985 $R_\odot$. The amount of periodic variation $(\Delta p/p)$ could be obtained using formula $\Delta p/p = A \times \sqrt{2[1-\cos(2\pi \times p/T)]}/p$ (Rovithis-Livaniou et al. 2000), where A is the amplitude of the sine function describing the period variation and T represents period of magnetic activity. As a result, we obtained $\Delta Q_1 = 6.10 \times 10^{48}$ g cm^2 for the primary component and $\Delta Q_2 = 2.27 \times 10^{48}$ g cm^2 for the secondary one. Nevertheless, the values of the quadrupole moments are both smaller than the typical values of active binaries ($10^{51} - 10^{52}$) (Lanza & Rodonò 1999). Because the quadrupole moments of VZ Lib are too small for active binaries, the period of oscillation might be caused by a third component. This result is not consistent with the result by statistical evaluation of the AIC value, as discussed in Section 3 of this paper. However, it is not sufficient to discard magnetic braking or a third body. Therefore, we cannot really distinguish between the magnetic activity or a third body as the cause for this period variation. However, Lu et al. (2001) pointed out that the companion of VZ Lib was itself a close binary. Hence, it required further radial velocity observations to distinguish whether VZ Lib is a triple or a quadruple system. This kind of phenomenon, the short period contact binary with a third body, was also found existing in other eclipsing binaries, such as AH Tauri, GN Boo and SS Ari (Table 8).

5.3 VZ Psc

For VZ Psc, our data showed an obvious O'Connell effect, namely, LCs of this system are highly asymmetric. The mass ratio is 0.81, consistent with that obtained by Hrivnak et al. (1995) through radial velocity study. The orbital inclination (i) is $56.3°$. The fractions of the primary star luminosity to the total luminosity are 0.8720 in B band, 0.8286 in V band, 0.7820 in R band and 0.7347 in I band. Potentials of the two components are 2.9982. The fillout factor (f) for VZ Psc is 95.7($\pm$ 0.25)%. Our orbital parameters indicate that there is a large difference between the temperatures in the two components of VZ Psc, about 900 K. Because the larger fillout would most likely lead to more mixing of the material in the envelope and tend to decrease the temperature difference, the large difference in temperature might be unfeasible. This peculiar combination of a large temperature difference and large fillout factor of VZ Psc was also found by other authors, as mentioned in Section 1. The larger difference in temperature was also found in previous work, such as 1120 K for FS Lupi (Milano et al. 1987) and about 900 K for BE Cep (Kaluzny 1986) and VZ Psc (Hrivnak & Milone 1989; Hrivnak et al. 1995). Some binaries like VZ Psc showing W Uma type properties have unequal depths of minima, and a component temperature difference often larger than 1000 K. There are several reasons (the evolution in the phase of broken contact, a particular distribution of coolspots on two stars at the primary minimum and an ellipsoidal variable) that could explain this phenomenon (e.g., Milano et al. 1987; Hrivnak & Milone 1989; Maceroni et al. 1990; Hrivnak et al. 1995). More observational data and better modeling would be required to fully explain it.

In summary, we have performed period analyses and photometric studies on binaries FG Sct, VZ Lib and VZ Psc. For FG Sct, this is the first time that we obtained its orbital parameters, and determined its orbital period variation and the mechanism causing this variation. For VZ Lib, we revised its orbital parameters and cyclic changes of orbital period. We compared our results with those from previous works and proposed possible mechanisms for the orbital period variations: potential presence of a third body (or bodies) or magnetic braking. For VZ Psc, we revised its orbital parameters and confirmed there is a large temperature difference between the two components. More observational data are necessary for more advanced modeling and to explore the whole parameter space with a Bayesian model in the future. We expanded details in the database of contact binaries by the three cases from this research.

Acknowledgements Our research was supported by the Joint Research Fund in Astronomy (U1631236 and U1431114) under cooperative agreement between the NSFC and CAS. LAMOST is operated and managed by NAOC. We acknowledge support from the staff at the Xinglong 60 cm and Lijiang 2.4 m telescopes. This work was partially supported by the Open Project Program of the Key Laboratory of Optical Astronomy, National Astronomical Observatories, Chinese Academy of Sciences. We would also like to thank Dr. Frank Levison for his generous financial support that enabled Butler University to join the SARA Consortium whose telescopes were used in carrying out part of the observations in this work.

References

Agerer, F., & Hubscher, J. 1996, Information Bulletin on Variable Stars, 4383
Agerer, F., & Huebscher, J. 1998, Information Bulletin on Variable Stars, 4606
Agerer, F., & Hubscher, J. 2002, Information Bulletin on Variable Stars, 5296
Akaike, H. 1974, IEEE Transactions on Automatic Control, 19, 716
Applegate, J. H. 1992, ApJ, 385, 621
Baştürk, Ö., Zola, S., Liakos, A., et al. 2015, New Astron., 41, 42
Barden, S. C. 1985, ApJ, 295, 162
Barone, F., Milano, L., Russo, G., & Sarna, M. J. 1989, Ap&SS, 159, 67
Bonnardeau, M. 2009, Journal of the American Association of Variable Star Observers (JAAVSO), 37, 137
Bradstreet, D. H. 1985, ApJS, 58, 413
Brat, L., Trnka, J., Smelcer, L., et al. 2011, Open European Journal on Variable Stars, 137, 1
Burnham, K. P., & Anderson, D. R. 2002, Model selection and inference: a practical information-theoretic approach (2nd edn.: Springer-Verlag)
Christopoulou, P.-E., Papageorgiou, A., Vasileiadis, T., & Tsantilas, S. 2012, AJ, 144, 149
Claria, J. J., & Lapasset, E. 1981, Information Bulletin on Variable Stars, 2035
Collier Cameron, A., Wilson, D. M., West, R. G., et al. 2007, MNRAS, 380, 1230
Copeland, H., Jensen, J. O., & Jorgensen, H. E. 1970, A&A, 5, 12
Covey, K. R., Ivezić, Ž., Schlegel, D., et al. 2007, AJ, 134, 2398
Cox, A. N. 2000, Allen's astrophysical quantities (New York: AIP Press; Springer)
Davidge, T. J., & Milone, E. F. 1984, Information Bulletin on Variable Stars, 2639
Demircan, O., Erdem, A., Ozdemir, S., et al. 2003, Information Bulletin on Variable Stars, 5364
Diethelm, R. 2006, Information Bulletin on Variable Stars, 5713
Diethelm, R. 2010, Information Bulletin on Variable Stars, 5945
Diethelm, R. 2011a, Information Bulletin on Variable Stars, 5992
Diethelm, R. 2011b, Information Bulletin on Variable Stars, 5960
Diethelm, R. 2012a, Information Bulletin on Variable Stars, 6029
Diethelm, R. 2012b, Information Bulletin on Variable Stars, 6011
Diethelm, R. 2013, Information Bulletin on Variable Stars, 6042
Dvorak, S. W. 2003, Information Bulletin on Variable Stars, 5378
Dvorak, S. W. 2006, Information Bulletin on Variable Stars, 5677
Eggen, O. J. 1967, ApJ, 150, L111
Erdem, A., & Öztürk, O. 2016, New Astron., 48, 33

Erkan, N., & Ulaş, B. 2016, New Astron., 46, 73
Fan, Y.-F., Bai, J.-M., Zhang, J.-J., et al. 2015, RAA (Research in Astronomy and Astrophysics), 15, 918
Hoffman, D. I., Harrison, T. E., McNamara, B. J., et al. 2006, AJ, 132, 2260
Hoffmeister, C. 1933, Astronomische Nachrichten, 247, 281
Hoňková, K., Juryšek, J., Lehký, M., et al. 2013, Open European Journal on Variable Stars, 160, 1
Honková, K., Juryšek, J., Lehký, M., et al. 2014, Open European Journal on Variable Stars, 165, 1
Hrivnak, B. J., & Milone, E. F. 1989, AJ, 97, 532
Hrivnak, B. J., Guinan, E. F., & Lu, W. 1995, ApJ, 455, 300
Hubscher, J., & Walter, F. 2007, Information Bulletin on Variable Stars, 5761
Hubscher, J., Steinbach, H.-M., & Walter, F. 2009, Information Bulletin on Variable Stars, 5889
Hubscher, J. 2013, Information Bulletin on Variable Stars, 6084
Hubscher, J. 2017, Information Bulletin on Variable Stars, 6196
Irwin, J. B. 1952, ApJ, 116, 211
Kaluzny, J. 1986, Acta Astronomica, 36, 121
Kazuo, K. 2013, VSOLJ Variable Star Bulletin, 55, 1
Krajci, T. 2006, Information Bulletin on Variable Stars, 5690
Kriwattanawong, W., Tasuya, O., & Poojon, P. 2016, New Astron., 44, 12
Kwee, K. K., & van Woerden, H. 1956, Bull. Astron. Inst. Netherlands, 12, 327
Lanza, A. F., Rodono, M., & Rosner, R. 1998, MNRAS, 296, 893
Lanza, A. F., & Rodonò, M. 1999, A&A, 349, 887
Lanza, A. F., & Rodonò, M. 2002, Astronomische Nachrichten, 323, 424
Lee, J. W., Kim, S.-L., Lee, C.-U., et al. 2013, ApJ, 763, 74
Li, K., Hu, S., Guo, D., et al. 2015, New Astron., 41, 17
Li, K., Hu, S.-M., Jiang, Y.-G., Chen, X., & Ren, D.-Y. 2014, New Astron., 30, 64
Liao, W.-P., Qian, S.-B., Zhao, E.-G., & Jiang, L.-Q. 2014, New Astron., 31, 65
Liu, L., Qian, S.-B., He, J.-J., Zhang, J., & Li, L.-J. 2009, Ap&SS, 321, 19
Lu, W., Rucinski, S. M., & Ogłoza, W. 2001, AJ, 122, 402
Lu, H.-p., Michel, R., Zhang, L.-y., & Castro, A. 2018, AJ, 156, 88
Lucy, L. B. 1967, ZAp, 65, 89
Luo, A.-L., Zhao, Y.-H., Zhao, G., et al. 2015, RAA (Research in Astronomy and Astrophysics), 15, 1095
Ma, S., Li, K., Li, Q.-C., & Gao, H.-Y. 2018, New Astron., 59, 1
Maceroni, C., van Hamme, W., & van't Veer, F. 1990, A&A, 234, 177
Marino, G., Arena, C., Bellia, I., et al. 2010, Information Bulletin on Variable Stars, 5917
Mayer, P. 1990, Bulletin of the Astronomical Institutes of Czechoslovakia, 41, 231
Milano, L., Russo, G., & Terzan, A. 1987, A&A, 183, 265
Milone, E. F., Hrivnak, B. J., & Fisher, W. A. 1985, AJ, 90, 354
Montes, D., Fernandez-Figueroa, M. J., de Castro, E., & Cornide, M. 1995, A&A, 294, 165
Nagai, K. 1999, VSOLJ Variable Star Bulletin, 33, 1
Nagai, K. 2001, VSOLJ Variable Star Bulletin, 38, 1
Nagai, K. 2002, VSOLJ Variable Star Bulletin, 39, 1
Nagai, K. 2003, VSOLJ Variable Star Bulletin, 40, 1
Nagai, K. 2004, VSOLJ Variable Star Bulletin, 42, 1
Nagai, K. 2005, VSOLJ Variable Star Bulletin, 43, 1
Nagai, K. 2006, VSOLJ Variable Star Bulletin, 44, 1
Nagai, K. 2007, VSOLJ Variable Star Bulletin, 45, 1
Nagai, K. 2008a, VSOLJ Variable Star Bulletin, 47, 1
Nagai, K. 2008b, VSOLJ Variable Star Bulletin, 46, 1
Nagai, K. 2009, VSOLJ Variable Star Bulletin, 48, 1
Nagai, K. 2010, VSOLJ Variable Star Bulletin, 50, 1
Nagai, K. 2011, VSOLJ Variable Star Bulletin, 51, 1
Nagai, K. 2012, VSOLJ Variable Star Bulletin, 53, 1
Nagai, K. 2014, VSOLJ Variable Star Bulletin, 56, 1
Nagai, K. 2015, VSOLJ Variable Star Bulletin, 59, 1
Nagai, K. 2016, VSOLJ Variable Star Bulletin, 61, 1
Nagai, K. 2017, VSOLJ Variable Star Bulletin, 63, 1
Nelson, R. H. 2004, Information Bulletin on Variable Stars, 5493
Noori, H. R., & Abedi, A. 2017, New Astron., 56, 5
Ogloza, W., Niewiadomski, W., Barnacka, A., et al. 2008, Information Bulletin on Variable Stars, 5843
Paschke, A., & Brat, L. 2006, Open European Journal on Variable Stars, 23, 13
Perryman, M. A. C., Lindegren, L., Kovalevsky, J., et al. 1997, A&A, 323, L49
Pi, Q.-F., Zhang, L.-Y., Li, Z.-M., & Zhang, X.-L. 2014, AJ, 147, 50
Pi, Q.-F., Zhang, L.-Y., Bi, S.-L., et al. 2017, AJ, 154, 260
Poretti, E. 1984, Information Bulletin on Variable Stars, 2487
Poretti, E. 1985, Information Bulletin on Variable Stars, 2671
Press, W. H., Teukolsky, S. A., Vetterling, W. T., & Flannery, B. P. 1992, Numerical Recipes in FORTRAN, The Art of Scientific Computing, (Cambridge Univ. Press, 2nd ed.)
Pribulla, T., & Rucinski, S. M. 2006, AJ, 131, 2986
Prša, A., & Zwitter, T. 2005, ApJ, 628, 426
Qian, S. B., Soonthornthum, B., Xiang, F. Y., Zhu, L. Y., & He, J. J. 2004, Astronomische Nachrichten, 325, 714
Qian, S.-B., Liao, W.-P., Liu, L., et al. 2008, New Astron., 13, 98
Qian, S.-B., He, J.-J., Zhang, J., et al. 2017, RAA (Research in Astronomy and Astrophysics), 17, 087
Qu, Z. N., Jiang, L. Q., Liu, J., et al. 2017, New Astronomy, 54, 103
Rovithis-Livaniou, H., Kranidiotis, A. N., Rovithis, P., & Athanassiades, G. 2000, A&A, 354, 904
Ruciński, S. M. 1969, Acta Astronomica, 19, 245
Rucinski, S. M., & Duerbeck, H. W. 2006, AJ, 132, 1539
Samec, R. G. 1989, PASP, 101, 661
Samec, R. G., & Bookmyer, B. B. 1987, Information Bulletin on Variable Stars, 2990
Samolyk, G. 2009, Journal of the American Association of Variable Star Observers (JAAVSO), 37, 44

Senavci, H. V., Tanriverdi, T., Torun, E., et al. 2007, Information Bulletin on Variable Stars, 5754

Singh, M., & Chaubey, U. S. 1986, Ap&SS, 124, 389

Skrutskie, M. F., Cutri, R. M., Stiening, R., et al. 2006, AJ, 131, 1163

Szalai, T., Kiss, L. L., Mészáros, S., Vinkó, J., & Csizmadia, S. 2007, A&A, 465, 943

Watanabe, T. 2000, VSOLJ Variable Star Bulletin, 37, 1

Watson, C. L. 2006, Journal of the American Association of Variable Star Observers (JAAVSO), 35, 318

West, A. A., Hawley, S. L., Walkowicz, L. M., et al. 2004, AJ, 128, 426

Wilson, R. E. 1979, ApJ, 234, 1054

Wilson, R. E. 1990, ApJ, 356, 613

Wilson, R. E. 1994, PASP, 106, 921

Wilson, R. E., & Devinney, E. J. 1971, ApJ, 166, 605

Wolff, S. C., Wallerstein, G., & Sandage, A. R. 1965, PASP, 77, 370

Xiang, F.-Y., Yu, Y.-X., & Xiao, T.-Y. 2015, AJ, 149, 62

Yang, Y., & Liu, Q. 2003, PASP, 115, 748

Yang, Y.-G., Dai, J.-M., Yin, X.-G., & Xiang, F.-Y. 2007, AJ, 134, 179

Yang, Y.-G., Lü, G.-L., Yin, X.-G., Zhu, C.-H., & Nakajima, K. 2009, AJ, 137, 236

Yang, Y.-G., Shao, Z.-Y., Pan, H.-J., & Yin, X.-G. 2011, PASP, 123, 895

Yang, Y.-G., Qian, S.-B., & Dai, H.-F. 2013, AJ, 145, 60

Yi, Z., Luo, A., Song, Y., et al. 2014, AJ, 147, 33

Yu, Y.-X., Zhang, X.-D., Hu, K., & Xiang, F.-Y. 2017, New Astron., 55, 13

Zejda, M. 2004, Information Bulletin on Variable Stars, 5583

Zejda, M., Mikulasek, Z., & Wolf, M. 2006a, Information Bulletin on Variable Stars, 5741

Zejda, M., Mikulasek, Z., & Wolf, M. 2006b, Information Bulletin on Variable Stars, 5741

Zhang, L.-Y., & Gu, S.-H. 2007, A&A, 471, 219

Zhang, X. B., & Zhang, R. X. 2007, MNRAS, 382, 1133

Zhang, L.-Y., Pi, Q.-f., & Yang, Y.-G. 2014, MNRAS, 442, 2620

Zhang, L.-Y., Yue, Q., Lu, H.-P., et al. 2017, RAA (Research in Astronomy and Astrophysics), 17, 105

Zhang, L., Lu, H., Han, X. L., et al. 2018, New Astron., 61, 36

Zhu, L., & Qian, S. 2006, MNRAS, 367, 423

Zola, S., Rucinski, S. M., Baran, A., et al. 2004, Acta Astronomica, 54, 299